VOL. 11, NO. 16, AUGUST 2016 ISSN 1819-6608
ARPN Journal of Engineering and Applied Sciences

www.arpnjournals.com

GRAPHENE: ELECTROCHEMICAL PRODUCTION AND ITS ENERGY STORAGE PROPERTIES

Gomaa A. M. Ali[1,2], Mashitah M. Yusoff[1] and Kwok Feng Chong[1]
[1]Faculty of Industrial Sciences & Technology, Universiti Malaysia Pahang, Gambang, Kuantan, Pahang, Malaysia
[2]Chemistry Department, Faculty of Science, Al–Azhar University, Assiut, Egypt
E-Mail: ckfeng@ump.edu.my

ABSTRACT

Graphene oxide was prepared by the Hummers' method and then electrochemically reduced to produce graphene nanosheets. Physicochemical characterizations were performed using XRD, FTIR, FESEM, TEM, Raman and UV-Vis techniques to elucidate the structure and morphology of the prepared material. The electrochemical study had been conducted on graphene by cyclic voltammetry, galvanostatic charge-discharge and impedance measurements, indicating its superb energy storage properties. The specific capacitance of graphene was 131 F g-1 at 0.1 A g-1. Impedance spectra showed low resistance of electrochemically produced graphene, supporting its suitability for energy storage applications, such as supercapacitor.

Keywords: electrochemical reduction graphene, supercapacitor cyclic voltammetry impedance.

INTRODUCTION

The capacitance properties of carbon materials are based on electrodouble layer (EDL) mechanism. In EDL supercapacitors, a double layer of electrolyte ions is formed on the surface of active materials. No charge transfer from chemical reactions in the electrode takes place. The charge distribution on the surface of the electrode depends on the porosity and the crystal structure of the electrode material. The EDL materials should have high surface area for high charge accumulation and a suitable pore structure to allow a rapid motion of the electrolyte ions (Endo *et al.*, 2001, Lota *et al.*, 2008). Different carbon materials have been studied for supercapacitors application such as activated carbon, carbon nanoparticles, carbon nanospheres, carbon nano-onion, carbon nanotubes and graphene (Ali *et al.*, 2014, Borgohain *et al.*, 2012, Lota *et al.*, 2008, Lota *et al.*, 2011, Stoller *et al.*, 2008, Tashima *et al.*, 2011).

Graphene is atomically thin two-dimensional (2D) system of sp2 carbon atoms organized in a hexagonal lattice structure so it exhibits many interesting electronic, optical and mechanical properties. The porous nature of graphene facilities ion transport processes, and therefore improves the performance of supercapacitors. Graphene has a large theoretical specific surface area (2630 m2 g−1), leading to high theoretical capacitance of 550 F g-1(Zhu *et al.*, 2010). Moreover, it has low electrical resistivity and long life time. Graphene can be prepared by chemical, electrochemical or thermal reduction of graphene oxide (Buglione *et al.*, 2012, Stoller *et al.*, 2008, Yang and Gunasekaran, 2013, Teo *et al.*, 2012). Electrochemical preparation is most provable as it is less time consuming as well as lower cost where no reducing agents are needed. Graphene has been prepared by chemical vapor deposition on Ni foam substrate and shows a specific capacitance of 55.3 F g-1 at 5 mV s-1 (Chen *et al.*, 2013). In addition, Cyclic voltammetry (CV) scanning was used to electrochemically reduce graphene oxide (GO) on glassy carbon electrode (Chen *et al.,* 2011, Yang and Gunasekaran, 2013). So far, there are no studies reported on the CV reduction of GO on Ni foam substrate. Reduction of GO on Ni foam (a few milligrams on 1 cm2) is an encouraging method, as it produce high amount of graphene and the electrode will be ready to be used as supercapacitor electrode directly without any further treatment or processing. Moreover, Ni foam provides high accessible surface area for loading materials with 3D porous network structure and acts as a current collector (Lu *et al.*, 2011).

In this work, reduced graphene oxide (rGO) was prepared by cyclic voltammetric reduction of the GO pasted on Ni foam electrode. The prepared material was characterized by XRD, FTIR, FESEM, TEM, Raman and UV-Vis techniques. The electrochemical properties were investigated using cyclic voltammetry, galvanostatic charge-discharge and electrochemical impedance spectroscopy.

EXPERIMENTAL PROCEDURES AND TECHNIQUES

Samples preparation

GO was synthesized by modified Hummers' method (Hummers and Offeman, 1958). Then GO was coated on Ni foam electrode. The electrochemical reduction process was performed in phosphate buffer solution pH 9 in potential window from 1.2 to 0 V vs. Ag/AgCl reference electrode for 500 cycles at 50 mV s-1.

Samples Characterization

The crystal structure was analyzed using a Rigaku X-ray diffractometer (Miniflex II with Cu-Kα radiation at 40 kV, 30 mA, λ = 1.5406 Å) within the 2 θ range of 5° to 80°. The functional groups were examined using a Perkin Elmer (Spectrum 100) infrared spectrophotometer over the range of 400–4000 cm-1. The UV tests were carried out using a Thermo Scientific (Genesys 10S) UV spectrophotometer at room temperature in the wavelength range from 200 to 900 nm. Raman

spectra were obtained using Raman Microscope (Invia, Renishaw, UK) with 532 nm laser excitation. The surface morphology was monitored by a JEOL (JSM-7800F) field emission scanning electron microscope (FESEM).

Electrochemical measurements

The electrochemical properties were measured in 5 M KOH as electrolyte using a 2-electrode configuration system (battery coin cell). The data were collected using an electrochemical workstation (Autolab/PGSTAT M101, Netherlands) equipped with a frequency response analyser. The potential was scanned between 0 and 1 V with different sweep rates between 2 and 100 mV s-1. Galvanostatic charge-discharge tests were performed at current density from 0.05 to 1 A g-1. Impedance data were collected from 500 kHz to 0.01 Hz, at open circuit potential (OCP) with an AC signal of 10 mV in amplitude.

RESULTS AND DISCUSSION

Structural and morphological analysis

Figure-1(a) shows XRD patterns for GO and rGO. GO shows a main peak located at 9.8° with a d-spacing of 9.43 Å. The large expansion of d-spacing of GO is usually ascribed to the insertion of oxygen-containing groups and H2O molecules (Ban *et al*., 2012). The other peak at 23° is detected and could be ascribed to the limited ordering of few–layers in GO. rGO shows a weak diffraction peak at 24.8° related to the (002) crystallographic plane of graphene structure (Tang *et al*., 2009). Disappearance of the 9.8° peak indicates that GO is reduced to rGO (El–Khodary *et al*., 2014). Three strong peaks related to Ni substrate were observed (Zhang *et al*., 2013).

Figure-1(b) shows the FTIR spectrum of rGO. The band at 1635 cm–1 is attributed to C=C stretching vibration (El–Khodary *et al*., 2014, Wang and Dou, 2012). The characteristic absorption bands of oxygen-contained groups, such as the intense band of O–H groups of adsorbed water appears at 3440 cm–1. The disappearance of 1740 cm–1 band confirms the reduction of the carbonyl groups in GO structure. The bands at 1400 and 1220 cm–1 is related to C–OH group and in-plane C=C, respectively due to skeletal stretching (El–Khodary *et al*., 2014).

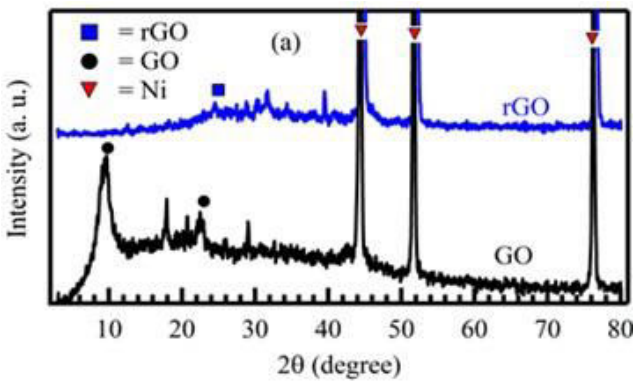

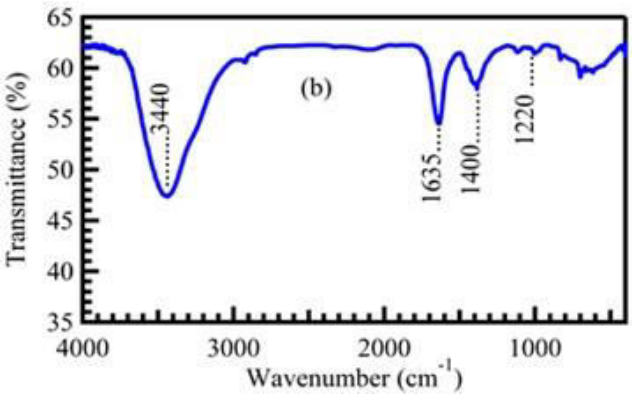

Figure-1. (a) XRD pattern of GO and rGO; (b) FTIR spectrum of rGO.

Further insights to the electronic conjugation of graphene can be obtained from UV–Vis absorption spectra as shown in Figure-2(a). The 275 nm peak indicates the restoration of π conjugation within graphene (Ali *et al*., 2015). No peaks at 230 nm or even the shoulder at 300 nm indicates the absence of C=O and GO is successfully reduced to graphene.

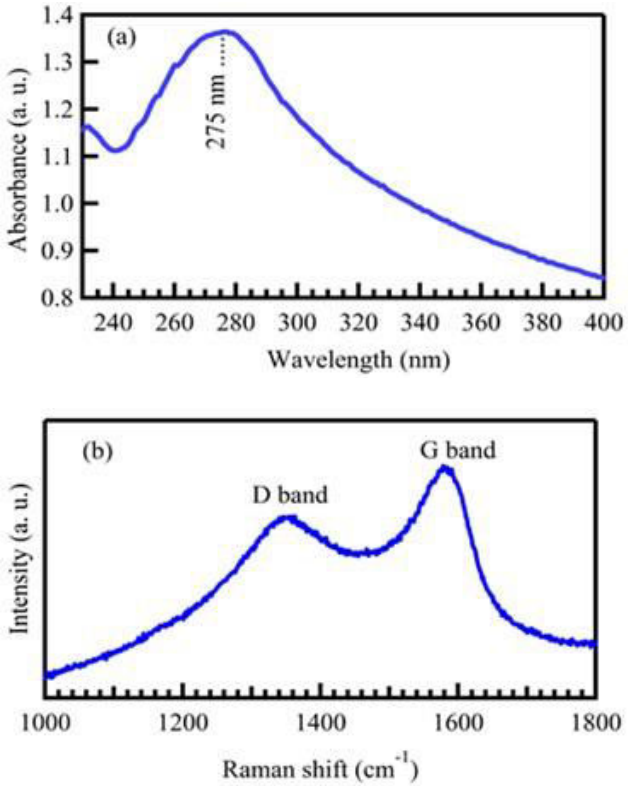

Figure-2. (a) UV-Vis and (b) Raman spectra of rGO.

Figure-2(b) shows the Raman spectra of rGO exhibiting *D* and *G* bands at 1347 cm^{-1} and 1586 cm^{-1}, respectively. The appearance of *D* band is a sign of disorder in the carbon lattice. The intensity ratio of *D* and *G* bands (I_D/I_G) is a measure of disorder, representing the sp^2/sp^3 carbon ratio. The I_D/I_G ratio for rGO is 0.85.

Similar Raman findings were reported elsewhere (El–Khodary *et al.*, 2014).

FESEM and TEM images of rGO are shown in Figure-3 (a) and (b) respectively. The findings indicate the nanosheets structure of graphene.

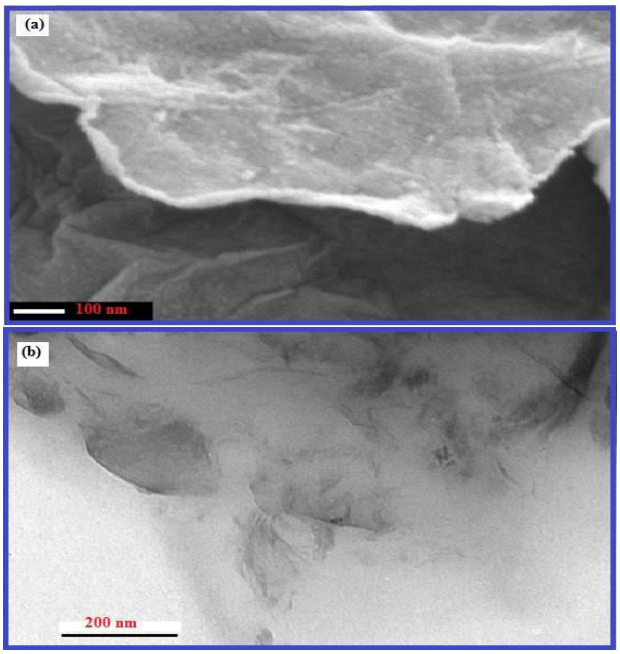

Figure-3. (a) FESEM and (b) TEM images of rGO.

Electrochemical properties

CV curves at different scan rates of rGO are shown in Figure-4. CV curves exhibit rectangular shape and symmetrical around zero, which reveals the ideal capacitive behavior of graphene.

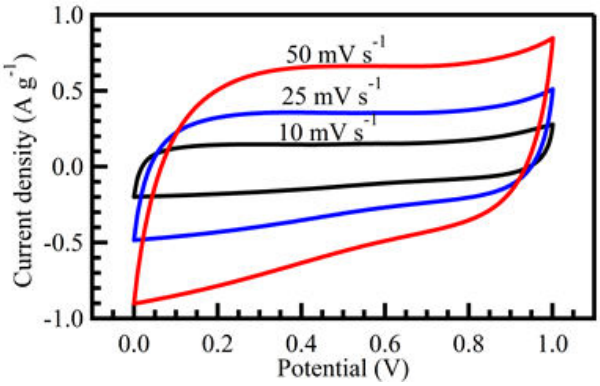

Figure-4. Cyclic voltammetry curves at different scan rates for rGO.

CV curves exhibit rectangular shape and symmetrical around zero, which reveals the ideal capacitive behavior of graphene. No redox peaks are observed, indicating electrochemical double layer capacitance and no pseudocapacitance takes place as a result of complete reduction of all oxygen groups of GO (Ali *et al.*, 2015, Buglione *et al.,* 2012, Kishore *et al.,* 2013, Stoller *et al.,* 2008).

The charge-discharge curves for rGO are shown in Figure-5(a). Linear charge and discharge curves with a neglected *iR* of less than 2% is obtained, indicating that the electrodes have low internal resistance which lead to better EDL performance. The specific capacitance was calculated from the slope of discharge curve according the equation reported elsewhere (Kishore *et al*., 2013, Ali *et al.*, 2014) and found to be 131 F g^{-1} at 0.1 A g^{-1}. This finding is very close to the reported for electrochemically reduced graphene (128 F g^{-1}) (Peng *et al.,* 2011) and higher than those for activated carbon (95 F g^{-1}) (Portet *et al*., 2005) and single-walled carbon nanotubes (90-120 F g^{-1}) (Kaempgen *et al.*, 2009). The electrochemical properties of hydrothermal reduction treatment of reduced GO on Ni foam using hydrazine hydrate (HrGO/NF) in KOH electrolyte have been reported (Xie and Zhan, 2015). HrGO/NF only shows 35 F g^{-1} at 1 A g^{-1}, while our electrochemically produced rGO shows around double of the specific capacitance. This is due to the sheet structure of graphene which facilitates the ions intercalation/de-intercalation rate (Ali *et al.,* 2015, Chen *et al.,* 2013).

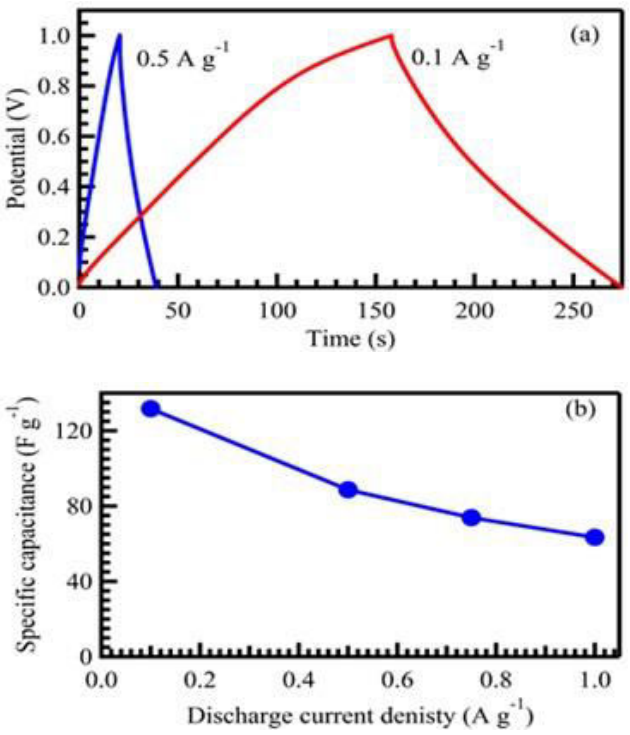

Figure-5. (a) Galvanostatic charge-discharge curves at the indicated current densities and (b) specific capacitance as a function of current density.

To study the electrical resistance of the prepared rGO, the electrochemical impedance spectroscopy (EIS) was conducted. Figure-6(a) shows Nyquist plot of rGO, which demonstrates a semicircle at high frequency region (see top inset) and straight line due to diffusion at low frequency region. The electrochemical parameters were

obtained by fitting the experimental data according to the equivalent fitting circuit as shown in the bottom inset of Figure-6(a).

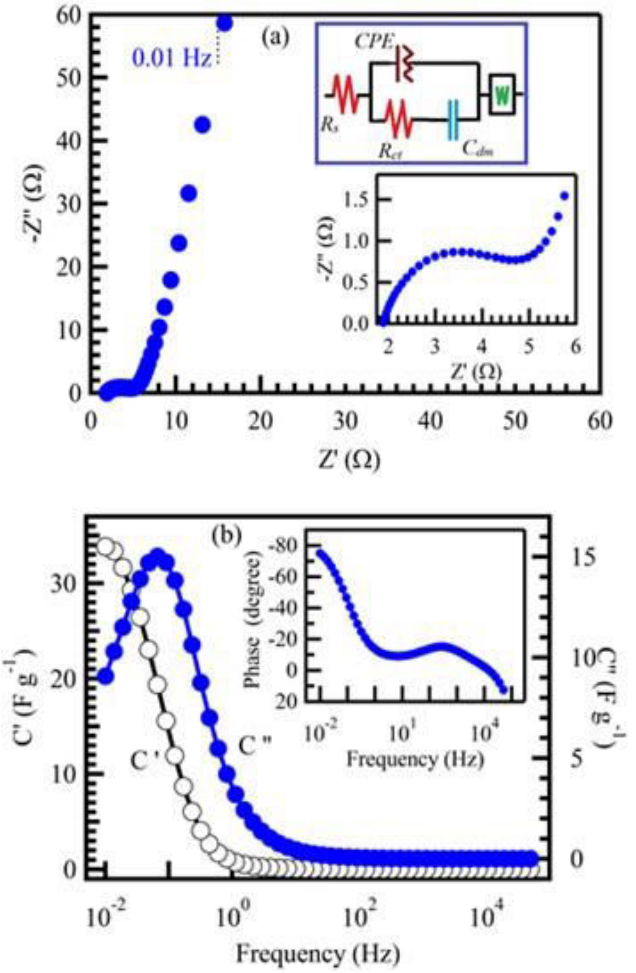

Figure-6. Nyquist plot (a) of ERGO at OCP, the insets are the zoomed high-frequency region of the plot and the equivalent circuit and (b) real and imaginary parts of the capacitance as functions of the frequency, the inset is Bode plot.

Electrochemically produced rGO shows a small solution (R_s) and charge transfer (R_{ct}) resistances of 1.82 and 3.13 Ω, respectively. R_{ct} is much lower than the reported values for electrochemically reduced graphene (29.7 Ω) (Yang and Gunasekaran, 2013) and vertically-oriented graphene (10 Ω) (Bo *et al.*, 2012), indicating the excellent power capabilities of graphene in this work. The real (C') and imaginary (C'') parts of the cell capacitance were calculated according to the equations reported elsewhere (Portet *et al.*, 2005) and presented in Figure 6(b). Bode plot shows the relationship between the phase angle and frequency of the rGO. It is seen that, the phase angle is -75˚ (see the inset of Figure 6(b)) which is close to the angle for ideal capacitor (-90˚) (Bo *et al.*, 2012). The relaxation time (τ) is calculated as: $\tau = 1/f_\circ$, where $f_\circ$ is the frequency at the maximum energy dissipation. τ was found to be 2.5 s, which is lower than this obtained for activated carbon (8 s) (Portet *et al.,* 2005). The electrochemical active specific surface area (S_E) was calculated as: $S_E = C_{dl}/C_d$, where, C_d is a constant value of 20 μF cm^{-2} (Chou *et al.*, 2006), C_{dl} was obtained from impedance data at low frequency (0.01 Hz) according to the equation $C_{\mathrm{dl}} = 1/(2\,\pi\, f \times m \times Z'')$, f is the frequency, Z'' is the imaginary part in the impedance, and m is the mass of the active material. The calculated value of S_E was found to be 45.6 m^2 g^{-1}. All electrochemical parameters are listed in table 1.

Table-1. Fitting parameters of the complex impedance experimental data.

R_s (Ω)	R_{ct} (Ω)	CPE (mF)	C_{dm} (mF)	S_E (m^2 g^{-1})	τ (s)
1.82	3.13	5.78	315	45.6	2.5

CONCLUSIONS

The work presents an electrochemical approach to produce graphene that possesses excellent structural and electrochemical properties. Its high specific capacitance and low resistance suggest it as a suitable material for supercapacitors application.

ACKNOWLEDGEMENTS

The authors would like to acknowledge the funding from the Ministry of Education Malaysia in the form of RACE fund RDU141309 and Ministry of Science, Technology and Innovation in the form of eScience fund RDU140501.

REFERENCES

[1] Ali, G.A.M., Makhlouf, S.A., Yusoff, M.M. and Chong, K.F. (2015). Structural and electrochemical characteristics of graphene nanosheets as supercapacitor electrodes. Reviews on Advanced Materials Science, 41(1), pp. 35–43.

[2] Ali, G.A.M., Manaf, S.A.B.A., Kumar, A., Chong, K.F. and Hegde, G. (2014). High performance supercapacitor using catalysis free porous carbon nanoparticles. Journal of Physics D–Applied Physics, 47, pp. 495307–495313.

[3] Ali, G.A.M., Tan, L.L., Jose, R., Yusoff, M.M. and Chong, K.F. (2014). Electrochemical performance studies of MnO2 nanoflowers recovered from spent battery. Materials Research Bulletin, 60, pp. 5-9.

[4] Ban, F.Y., Majid, S.R., Huang, N.M. and Lim, H.N. (2012). Graphene oxide and its electrochemical performance. International Journal of Electrochemical Science, 7, pp. 4345–4351.

[5] Bo, Z., Wen, Z., Kim, H., Lu, G., Yu, K. and Chen, J. (2012). One–step fabrication and capacitive behavior of electrochemical double layer capacitor electrodes using vertically–oriented graphene directly grown on metal. Carbon, 50(12), pp. 4379–4387.

[6] Borgohain, R., Li, J., Selegue, J.P. and Cheng, Y.T. (2012). Electrochemical study of functionalized carbon nano–onions for high-performance supercapacitor electrodes. The Journal of Physical Chemistry C, 116(28), pp. 15068–15075.

[7] Buglione, L., Chng, E.L.K., Ambrosi, A., Sofer, Z. and Pumera, M. (2012). Graphene materials preparation methods have dramatic influence upon their capacitance. Electrochemistry Communications, 14(1), pp. 5–8.

[8] Chen, L., Tang, Y., Wang, K., Liu, C. and Luo, S. (2011). Direct electrodeposition of reduced graphene oxide on glassy carbon electrode and its electrochemical application. Electrochemistry Communications, 13(2), pp. 133–137.

[9] Chen, W., Fan, Z., Zeng, G. and Lai, Z. (2013). Layer–dependent supercapacitance of graphene films grown by chemical vapor deposition on nickel foam. Journal of Power Sources, 225, pp. 251–256.

[10] Chou, S., Cheng, F. and Chen, J. (2006). Electrodeposition synthesis and electrochemical properties of nanostructured γ–MnO2 films. Journal of Power Sources, 162(1), pp. 727–734.

[11] El–Khodary, S.A., El–Enany, G.M., El–Okr, M. and Ibrahim, M. (2014). Preparation and characterization of microwave reduced graphite oxide for high–performance supercapacitors. Electrochimica Acta, 150, pp. 269–278.

[12] Endo, M., Takeda, T., Kim, Y.J., Koshiba, K. and Ishii, K. (2001). High power electric double layer capacitor (EDLC's); from operating principle to pore size control in advanced activated carbons. Carbon Science, 1(2-3), pp. 117–128.

[13] Hummers, W.S. and Offeman, R.E. (1958). Preparation of graphitic oxide. Journal of the American Chemical Society, 80(6), pp. 1339–1339.

[14] Kaempgen, M., Chan, C.K., Ma, J., Cui, Y. and Gruner, G. (2009). Printable thin film supercapacitors using single–walled carbon nanotubes. Nano Letters, 9(5), pp. 1872–1876.

[15] Kishore, M.S., Srimathi, P., Kumar, S., Addepalli, S., Swaminathan, S., Tilak, V. and Colborn, R. (2013). Combustion synthesis of graphene and ultracapacitor performance. Bulletin of Materials Science, 36(4), pp. 667–672.

[16] Lota, G., Centeno, T.A., Frackowiak, E. and Stoeckli, F. (2008). Improvement of the structural and chemical properties of a commercial activated carbon for its application in electrochemical capacitors. Electrochimica Acta, 53(5), pp. 2210–2216.

[17] Lota, G., Fic, K. and Frackowiak, E. (2011). Carbon nanotubes and their composites in electrochemical applications. Energy & Environmental Science, 4(5), pp. 1592–1605.

[18] Lu, Z.Y., Chang, Z., Zhu, W. and Sun, X.M. (2011). Beta–phased Ni(OH)2 nanowall film with reversible capacitance higher than theoretical Faradic capacitance. Chemical Communications, 47(34), pp. 9651–9653.

[19] Peng, X.Y., Liu, X.X., Diamond, D. and Lau, K.T. (2011). Synthesis of electrochemically–reduced graphene oxide film with controllable size and thickness and its use in supercapacitor. Carbon, 49(11), pp. 3488–3496.

[20] Portet, C., Taberna, P.L., Simon, P., Flahaut, E. and Laberty–Robert, C. (2005). High power density electrodes for Carbon supercapacitor applications. Electrochimica Acta, 50(20), pp. 4174–4181.

[21] Stoller, M.D., Park, S., Zhu, Y., An, J. and Ruoff, R.S. (2008). Graphene–based ultracapacitors. Nano Letter, 8(10), pp. 3498–3502.

[22] Tang, L., Wang, Y., Li, Y., Feng, H., Lu, J. and Li, J. (2009). Preparation, structure, and electrochemical properties of reduced graphene sheet films. Advanced Functional Materials, 19(17), pp. 2782–2789.

[23] Tashima, D., Yamamoto, E., Kai, N., Fujikawa, D., Sakai, G., Otsubo, M. and Kijima, T. (2011). Double layer capacitance of high surface area carbon nanospheres derived from resorcinol–formaldehyde polymers. Carbon, 49(14), pp. 4848–4857.

[24] Teo, E.Y.L., Tan, L.L., Chong, K.F. (2012). Facile corrosion protection coating from graphene. International Journal of Chemical Engineering and Applications, 3(6), pp. 454-455.

[25] Wang, X. and Dou, W. (2012). Preparation of graphite oxide (GO) and the thermal stability of silicone rubber/GO nanocomposites. Thermochimica Acta, 529, pp. 25–28.

[26] Xie, Y. and Zhan, Y. (2015). Electrochemical capacitance of porous reduced graphene oxide/nickel foam. Journal of Porous Materials, 22(2), pp. 403–412.

[27] Yang, J. and Gunasekaran, S. (2013). Electrochemically reduced graphene oxide sheets for use in high performance supercapacitors. Carbon, 51, pp. 36–44.

[28] Zhang, H., Zhang, X., Zhang, D., Sun, X., Lin, H., Wang, C. and Ma, Y. (2013). One–step electrophoretic deposition of reduced graphene oxide and Ni(OH)2 composite films for controlled syntheses supercapacitor electrodes. The Journal of Physical Chemistry B, 117(6), pp. 1616–1627.

[29] Zhu, Y., Murali, S., Cai, W., Li, X., Suk, J.W., Potts, J.R. and Ruoff, R.S. (2010). Graphene and graphene oxide: synthesis, properties, and applications. Advanced Materials, 22(35), pp. 3906–3924.